



# Increasing atmospheric helium due to fossil fuel exploitation

Benjamin Birner <sup>®</sup> ✓, Jeffrey Severinghaus, Bill Paplawsky and Ralph F. Keeling <sup>®</sup>

Fossil fuels contain small amounts of helium, which are co-released into the atmosphere together with carbon dioxide. However, a clear build-up of helium in the atmosphere has not previously been detected. Using a high-precision mass spectrometry technique to determine the atmospheric ratio of helium-4 to nitrogen, we show that helium-4 concentrations have increased significantly over the past five decades. Obtaining a direct measure of the rise in atmospheric helium-4 is possible because changes in nitrogen are negligible. Using 46 air samples acquired between 1974 and 2020, we find that the helium-4 concentration increased at an average rate of  $39\pm3$  billion mol per year ( $2\sigma$ ). Given that previous observations have shown that the ratio between helium-3 and helium-4 in the atmosphere has remained constant, our results also imply that the concentration of helium-3 is increasing. The inferred rise in atmospheric helium-3 greatly exceeds estimates of anthropogenic emissions from natural gas, nuclear weapons and nuclear power generation, suggesting potential problems with previous isotope measurements or an incorrect assessment of known sources.

atural gas is enriched in <sup>4</sup>He from radioactive decay of thorium and uranium in Earth's crust. Anthropogenic fossil fuel usage has therefore greatly increased the release of crustal <sup>4</sup>He to the atmosphere over the natural background rate<sup>1-10</sup>. By contrast, most natural gas sources are thought to be less enriched in <sup>3</sup>He. The extraction of natural gas is thus expected to increase the <sup>4</sup>He abundance of air while decreasing the <sup>3</sup>He/<sup>4</sup>He ratio<sup>1-10</sup>.

Studies of atmospheric <sup>3</sup>He/<sup>4</sup>He over the past four decades have yielded conflicting results. Early observations<sup>1,11,12</sup>, studies based on air trapped in ceramics and metallurgical slags<sup>6,7,13</sup>, and global helium budget calculations<sup>2,7,10</sup> support the existence of an anthropogenic signal, whereas several independent measurements with improved error margins recently constrained any atmospheric <sup>3</sup>He/<sup>4</sup>He trend to be indistinguishable from zero<sup>3,4,14,15</sup>. However, the precision of helium isotope measurements is currently limited to about 1‰ per sample due to the low abundance of the rare isotope <sup>3</sup>He in the atmosphere. Furthermore, other sources of <sup>3</sup>He could partly offset the decline of <sup>3</sup>He/<sup>4</sup>He from fossil fuel extraction<sup>4,15</sup>.

In this Article, we present high-precision measurements of the  ${}^{4}$ He to  $N_{2}$  ratio in archived air samples, which improve the ability to detect the  ${}^{4}$ He build-up by almost two orders of magnitude owing to the higher and more stable abundance of  $N_{2}$  than  ${}^{3}$ He. Results are reported in delta notation (that is, as  $\delta({}^{4}$ He/ $N_{2}$ ); see Methods).

# Atmospheric He/N, rise

We analysed 46 air samples collected at Scripps Institution of Oceanography (California, USA), Trinidad Head (California, USA) and Cape Grim (Australia) between 1974 and 2020. Samples were pumped into high-pressure aluminium cylinders, chrome–molybdenum steel cylinders or 341 stainless steel 'Essex tanks' (Essex Cryogenics) using different pumping systems (Methods). Samples were screened for leakage during storage and corrected for a small artefactual fractionation caused during sample collection (Methods). The 'He/N<sub>2</sub> was measured using a mass spectrometric technique that relies on measuring 'He in a continuous pressure-stabilized flow of air that has had all non-noble gases removed using a hot titanium getter. The method effectively determines relative differences

in the helium mole fraction between sample and standard air, which are combined with information from separate measurements of  $O_2/N_2$ ,  $Ar/N_2$  and  $CO_2$  to calculate  $^4He/N_2$   $^{16}$ . Reporting the  $^4He/N_2$  rather than the helium mole fraction directly is desirable because  $N_2$  has remained stable in the atmosphere to within 0.01% over the past decades while the overall composition of the atmosphere has changed  $^{16}$ . Accounting for uncertainty in the fractionation correction and supplementary gas data, we estimate an overall analytical uncertainty of 0.07% ( $2\sigma$ ) for the  $^4He/N_2$  measurement (Methods).

The results (Fig. 1) show that the observed change in atmospheric  $^4\text{He/N}_2$  between 1974 and 2020 is  $1.93\pm0.14\%e$ , corresponding to an average increase of  $0.042\pm0.003\%e$  yr  $^1$  ( $2\sigma$  error from bootstrapping) or  $39\pm3$  billion mol of  $^4\text{He}$  (atmospheric  $^4\text{He}$  inventory:  $9.268\times10^{14}\,\text{mol}$ ). The  $^4\text{He}$  build-up accelerates and reaches  $\sim\!50-53\,\text{billion}\,\text{mol}\,\text{yr}^{-1}$  between 2010 and 2014. This is two orders of magnitude greater than fluxes in the natural background state characterized by slow crustal degassing and He escape to space  $^{8,10,17,18}$  so must be anthropogenic in origin. The trend is generally lower than the estimated anthropogenic impact in global inventories of  $^4\text{He}$  emissions  $^{2,7,10}$ .

The results also show shorter-term variability of uncertain origin. The spread of Essex tank data around a best-fit line is about two times larger than expected from the analytical uncertainty alone; the spread of data points from chrome-molybdenum steel cylinders is even higher, in particular before the year 2000. While the short-term variability in the Essex tanks could result from real atmospheric variability, the much greater variability in data from steel cylinders is almost certainly an artefact, which could be related to undocumented differences in the agent used to dry the air samples. For example, 13X molecular sieve was probably used for some steel cylinders before 2000, and laboratory tests suggest an associated risk of fractionation (Extended Data Fig. 2). Essex tanks, by contrast, were never subject to any chemical purification and thus provide a higher fidelity record. Despite the short-term variability, agreement between Essex tanks and high-pressure cylinders is good, and results from tank G-038 filled at Cape Grim in 1995 on a different pumping system agree with the observations from the Northern Hemisphere.

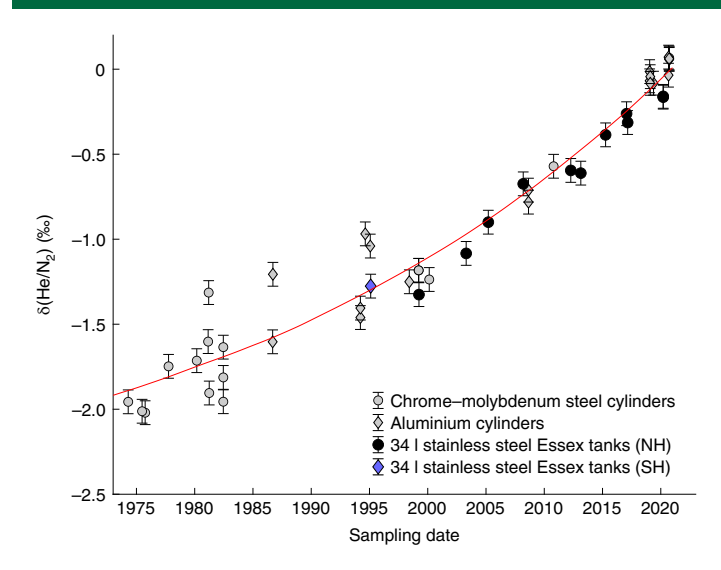


**Fig. 1** | Atmospheric <sup>4</sup>He/N<sub>2</sub> change relative to the average of samples in 2020. Data are shown from high-pressure chrome–molybdenum steel cylinders (grey circles), aluminium cylinders (grey diamonds), 34 l stainless steel Essex tanks filled in the Northern Hemisphere (NH, black circles) and one Essex tank filled at Cape Grim in the Southern Hemisphere (SH, blue diamond) with  $2\sigma$  error bars. Using independent observations of δ(Ar/N<sub>2</sub>), grey data points were corrected for a small bias introduced during sampling (Methods). The best-fit line (red) is obtained by scaling global cumulative natural gas emissions (Extended Data Fig. 1) by a constant while maintaining the curvature of the emissions trend. The observed atmospheric build-up implies a mean helium content of  $0.03\pm0.002\%$  in natural gas assuming other fossil fuel contributions to the trend are negligible<sup>2</sup>. Uncertainty about the effective sampling date for mixtures of air from multiple days (see Supplementary Table 1) is smaller than the size of the data points.

This shows that our samples are unlikely to be affected by helium leakage and that we reliably capture a global signal.

If we assume that helium emissions are tied to natural gas emission, we can quantify the average helium content of natural gas globally. In Fig. 1, we fit a trendline to the atmospheric  $^4{\rm He/N_2}$  history that is directly proportional to the cumulative global natural gas emissions from (1) natural gas production, (2) flaring and (3) fugitive fossil methane emissions (Extended Data Fig. 1). This fit, which largely explains the observed acceleration, yields a constant scale factor that corresponds to a mean  $^4{\rm He}$  content of  $0.030\pm0.002\%$  in natural gas (mol  $^4{\rm He}$  per mol C). Our estimate of cumulative natural gas emissions in Extended Data Fig. 1 presumably already accounts for a large fraction of helium release associated with oil and coal because helium will be found primarily in the gas fraction, that is, associated petroleum gas or coalbed methane. In addition, ref.  $^2$  showed that coal probably makes a negligible contribution to overall helium emissions due to its young age and insufficient uranium content.

Incidentally, the measured global  $^4$ He build-up vastly exceeds the helium released from commercial use in manufacturing, research and medical equipment. Commercial helium production from 2010 to 2014 was  $5-8\times10^9$  mol yr<sup>-1</sup> (refs.  $^{4,19}$ ), thus accounting for only 9–15% of the observed helium trend.

We are not aware of any other processes that contribute substantially to the  ${}^4\text{He/N}_2$  trend. On the basis of representative helium content of groundwater and anthropogenic water usage, we estimate that the effect of human groundwater use on  $\text{He/N}_2$  is very small. Helium concentrations in groundwater typically fall between  $10^{-8}$  and  $10^{-5}$  cm<sup>3</sup> (STP He) cm<sup>-3</sup> (H<sub>2</sub>O) depending on the age of the water and geological setting $^{20-23}$ . Human groundwater usage was  $952 \, \text{km}^3 \, \text{yr}^{-1}$  in  $2010^{24}$ , which places an upper limit on the degassing

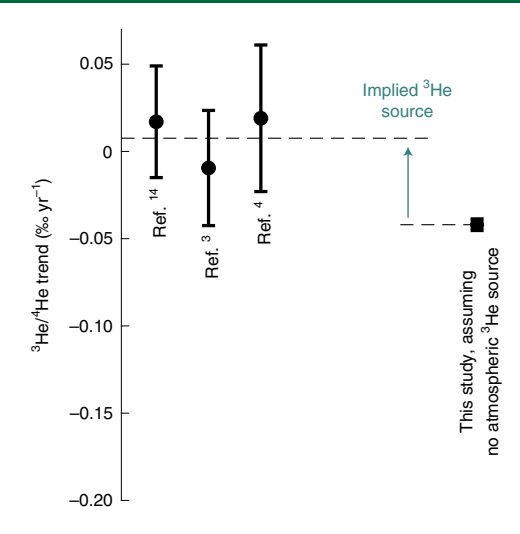


**Fig. 2 | Atmospheric**  ${}^3\text{He}/{}^4\text{He}$  trend and inferred  ${}^3\text{He}$  emissions. The observed trend in atmospheric  ${}^3\text{He}/{}^4\text{He}$  is compared with a  ${}^3\text{He}/{}^4\text{He}$  trend calculated from our  ${}^4\text{He}/{}^1\text{N}_2$  measurements assuming no  ${}^3\text{He}$  was added to the atmosphere simultaneously. Dashed lines show the variance-weighted mean trends, and error bars are  $2\sigma$  uncertainties. The discrepancy between the measurements implies an atmospheric  ${}^3\text{He}$  build-up of  $49 \pm 20$  per meg yr $^{-1}$ .

of helium from extracted groundwater of around  $4.3 \times 10^8 \,\mathrm{mol}\,\mathrm{yr}^{-1}$  or  $0.46\,\mathrm{per}\,\mathrm{meg}\,\mathrm{yr}^{-1}$ . The impact from natural degassing of fossil groundwater that has accumulated crustal He in regions previously frozen during the last glacial period is similarly negligible<sup>5,7</sup>. Ref. <sup>25</sup> recently discussed a stratospheric influence on tropospheric <sup>4</sup>He/N<sub>2</sub> via changing circulation. However, any such long-term variability is probably smaller than  $0.5\,\mathrm{per}\,\mathrm{meg}\,\mathrm{yr}^{-1}$ .

# Atmospheric 3He

In conjunction with previous studies of changes in atmospheric  ${}^{3}\text{He}/{}^{4}\text{He}$ , the observed  ${}^{4}\text{He}/{}^{2}$  trend may put important constraints on the release of  ${}^{3}\text{He}$  to the atmosphere (Fig. 2). We average three independent observations of the  ${}^{3}\text{He}/{}^{4}\text{He}$  trend ${}^{3,4,14}$ , weighing them by variance, which yields a change of  ${}^{+}8\pm20\,\text{per}\,\text{meg}\,\text{yr}^{-1}$  over the past century ( ${}^{2}\sigma$ ). To simultaneously satisfy both observational constraints, a rise of  ${}^{3}\text{He}/{}^{3}\text{Le}$  by  ${}^{4}9\pm20\,\text{per}\,\text{meg}\,\text{yr}^{-1}$  is needed, which is equivalent to an additional release of about  ${}^{6}3,000\pm25,000\,\text{mol}\,\text{yr}^{-1}$   ${}^{3}\text{He}$  into the atmosphere (atmospheric  ${}^{3}\text{He}$  inventory:  ${}^{1}.27\times10^{9}\,\text{mol}$ ).

A key question is whether the implied <sup>3</sup>He build-up is real and, if so, how to explain it. We briefly explore three possibilities: (1) the observations used to determine the atmospheric <sup>3</sup>He/<sup>4</sup>He are incorrect, (2) the <sup>3</sup>He content of natural gas is greater than previously thought and (3) there is an additional, unknown source of <sup>3</sup>He.

In the absence of an atmospheric  ${}^{3}$ He source,  ${}^{3}$ He/ ${}^{4}$ He should be decreasing at a rate of  $0.042\pm0.003\%e$  yr $^{-1}$ . This seems improbable given that recent data from three independent studies agree and show no significant helium isotope trend (Fig. 2). The three selected studies represent the most recent high-precision investigations of the helium isotope trend and are based exclusively on samples stored in metal containers, which addresses concerns about previous observations regarding limited analytical precision $^{5}$ , fractionation, helium leakage, and in situ helium production $^{6,7}$ . However, there is some contradictory evidence published previously by other authors $^{1,6,7,12,13}$ , and we cannot completely rule out that atmospheric helium isotope ratios are declining.

The <sup>3</sup>He/<sup>4</sup>He observations could be explained if natural gas in fact had a <sup>3</sup>He/<sup>4</sup>He ratio 1.18±0.49 times greater than in the atmosphere. Such a high ratio cannot be completely ruled out as the <sup>3</sup>He/<sup>4</sup>He ratio of helium in natural gas is poorly known globally and

can vary greatly between different wells<sup>26–29</sup>. The ratio depends on the presence of mantle-derived primordial helium as well as the mineralogical composition of the gas's source region, that is, the relative abundances of lithium-, uranium- and thorium-containing minerals, which produce  $^3$ He and  $^4$ He in decay reactions. Although the issue is not settled, published studies on He isotopes have generally assumed a much lower ratio in fossil fuels<sup>1–6,30</sup>, as expected from the low average  $^3$ He/ $^4$ He ratio of  $1.08 \times 10^{-8}$  in Earth's upper crust $^{31}$ .

The implied <sup>3</sup>He increase constitutes a recent perturbation on top of the steady-state natural degassing of <sup>3</sup>He into the atmosphere, which has been estimated to be an order of magnitude smaller<sup>8</sup>. Known anthropogenic sources include production from tritium decay (half-life of 12.3 years) in the nuclear weapons stockpile, energy production and atmospheric weapons testing. These tritium sources alone, however, are insufficient to explain the observed helium trend, and tritium release is heavily monitored. The continuous production from the nuclear stockpile and the historic input from nuclear weapons testing average over the past six decades to an annual input of roughly 2,000–4,000 mol yr<sup>-1</sup>, which is more than an order of magnitude smaller than the implied atmospheric <sup>3</sup>He build-up<sup>4</sup>. To date, cumulative production of tritium in pressurized heavy-water reactors has probably been less than the tritium added by atmospheric weapons testing<sup>32</sup>.

Overall, this presents a major puzzle in the <sup>3</sup>He budget, which motivates a search for missing <sup>3</sup>He sources on Earth, especially since <sup>3</sup>He is considered an important, yet scarce, resource<sup>33</sup>.

# **Summary and conclusions**

Measurements of the  ${}^4\text{He/N}_2$  ratio in 46 high-pressure samples of archived old air using a new mass spectrometric technique<sup>25</sup> reveal an atmospheric build-up of  ${}^4\text{He}$  of  $0.042\pm0.003\%$  yr $^{-1}$  ( $2\sigma$ ), or  $39\pm3$  billion mol yr $^{-1}$ , between 1974 and 2020. The atmospheric rise of  ${}^4\text{He/N}_2$  accelerates from roughly 0.020 to 0.065% y $^{-1}$  over the record, matching the exponential rise in fossil fuel exploitation. Assuming that helium release associated with natural gas emissions and combustion is the primary cause of the observed trend implies a mean helium content in natural gas of  $0.030\pm0.002\%$ , which is an order of magnitude less than commonly used estimates<sup>2,34</sup>. A comparison of our results with previous observations of a near-zero trend in atmospheric  ${}^3\text{He}/{}^4\text{He}^{3,4,14}$  suggests a so far unidentified source of the scarce resource  ${}^3\text{He}$ .

# Online content

Any methods, additional references, Nature Research reporting summaries, source data, extended data, supplementary information, acknowledgements, peer review information; details of author contributions and competing interests; and statements of data and code availability are available at https://doi.org/10.1038/s41561-022-00932-3.

Received: 15 February 2021; Accepted: 16 March 2022; Published online: 9 May 2022

## References

- Sano, Y., Wakita, H., Makide, Y. & Tominaga, T. A ten-year decrease in the atmospheric helium isotope ratio possibly caused by human activity. *Geophys. Res. Lett.* 16, 1371–1374 (1989).
- Oliver, B. M., Bradley, J. G. & Farrar, H. IV Helium concentration in the Earth's lower atmosphere. *Geochim. Cosmochim. Acta* 48, 1759–1767 (1984).
- Mabry, J. C. et al. No evidence for change of the atmospheric helium isotope composition since 1978 from re-analysis of the Cape Grim Air Archive. Earth Planet. Sci. Lett. 428, 134–138 (2015).
- Boucher, C., Marty, B., Zimmermann, L. & Langenfelds, R. Atmospheric helium isotopic ratio from 1910 to 2016 recorded in stainless steel containers. *Geochem. Perspect. Lett.* 6, 23–27 (2018).
- Brennwald, M. S. et al. Concentrations and isotope ratios of helium and other noble gases in the Earth's atmosphere during 1978–2011. Earth Planet. Sci. Lett. 366, 27–37 (2013).

 Sano, Y., Furukawa, Y. & Takahata, N. Atmospheric helium isotope ratio: possible temporal and spatial variations. *Geochim. Cosmochim. Acta* 74, 4893–4901 (2010).

- Pierson-Wickmann, A. C., Marty, B. & Ploquin, A. Helium trapped in historical slags: a search for temporal variation of the He isotopic composition of air. *Earth Planet. Sci. Lett.* 194, 165–175 (2001).
- Torgersen, T. Terrestrial helium degassing fluxes and the atmospheric helium budget: implications with respect to the degassing processes of continental crust. Chem. Geol. 79, 1–14 (1989).
- 9. Banks, P. M. & Kockarts, G. Aeronomy Part B 1st edn (Academic Press, 1973).
- 10. Sano, Y., Marty, B. & Burnard, P. in *The Noble Gases as Geochemical Tracers* 2nd edn (ed. Burnard, P.) 17–31 (Springer, 2013).
- Sano, Y., Wakita, H., Makide, Y. & Tominaga, T. Reply to Lupton and Graham. Geophys. Res. Lett. 18, 486–4888 (1991).
- Mishima, K. et al. Accurate determination of the absolute <sup>3</sup>He/<sup>4</sup>He ratio of a synthesized helium standard gas (Helium Standard of Japan, HESJ): toward revision of the atmospheric <sup>3</sup>He/<sup>4</sup>He ratio. *Geochem. Geophys. Geosyst.* 19, 3995–4005 (2018).
- Matsuda, J. I., Matsumoto, T. & Suzuki, A. Helium in old porcelain: the historical variation of the He isotopic composition in air. *Geochem. J.* 44, 5–9 (2010).
- Lupton, J. & Evans, L. Changes in the atmospheric helium isotope ratio over the past 40 years. Geophys. Res. Lett. 40, 6271–6275 (2013).
- Lupton, J. & Evans, L. The atmospheric helium isotope ratio: is it changing? Geophys. Res. Lett. 31, L13101 (2004).
- Birner, B., Paplawsky, W., Severinghaus, J. & Keeling, R. F. A method for resolving changes in atmospheric He/N<sub>2</sub> as an indicator of fossil fuel extraction and stratospheric circulation. *Atmos. Meas. Tech.* 14, 2515–2527 (2021).
- Kockarts, G. Helium in the terrestrial atmosphere. Space Sci. Rev. 14, 723–757 (1973).
- Torgersen, T. Continental degassing flux of <sup>4</sup>He and its variability. Geochem. Geophys. Geosyst. 11, Q06002 (2010).
- Mohr, S. & Ward, J. Helium production and possible projection. *Minerals* 4, 130–144 (2014).
- Datta, P. S. et al. A survey of helium in ground water in parts of Sabarmati basin in Gujarat state and in the Jaisalmer district, Rajasthan. *Hydrol. Sci.* Bull. 25, 183–193 (1980).
- Kulongoski, J. T., Hilton, D. R., Cresswell, R. G., Hostetler, S. & Jacobson, G. Helium-4 characteristics of groundwaters from Central Australia: comparative chronology with chlorine-36 and carbon-14 dating techniques. *J. Hydrol.* 348, 176–194 (2008).
- Kulongoski, J. T., Hilton, D. R. & Izbicki, J. A. Source and movement of helium in the eastern Morongo groundwater basin: the influence of regional tectonics on crustal and mantle helium fluxes. *Geochim. Cosmochim. Acta* 69, 3857–3872 (2005).
- Torgersen, T. & Clarke, W. B. Helium accumulation in groundwater, I: an evaluation of sources and the continental flux of crustal <sup>4</sup>He in the Great Artesian Basin, Australia. *Geochim. Cosmochim. Acta* 49, 1211–1218 (1985).
- Wada, Y. & Bierkens, M. F. Sustainability of global water use: past reconstruction and future projections. *Environ. Res. Lett.* 9, 104003 (2014).
- Birner, B. et al. Gravitational separation of Ar/N<sub>2</sub> and age of air in the lowermost stratosphere in airborne observations and a chemical transport model. Atmos. Chem. Phys. 20, 12391–12408 (2020).
- Aldrich, L. T. & Nier, A. O. The occurrence of He<sup>3</sup> in natural sources of helium. *Phys. Rev.* 74, 1590–1594 (1948).
- Davidson, T. A. & Emerson, D. E. Method and Apparatus for Direct Determination of Helium-3 in Natural Gas and Helium (US Department of the Interior, 1990).
- Wittenberg, L. J. Inventory of terrestrial helium-3. In Abstracts Presented to the Topical Conference Origin of the Earth 109–110 (Lunar and Planetary Institute, 1988).
- Sano, Y., Tominaga, T., Nakamura, Y. & Wakita, H. <sup>3</sup>He/<sup>4</sup>He ratios of methane-rich natural gases in Japan. *Geochem. J.* 16, 237–245 (1982).
- Pinti, D. L. & Marty, B. in Fluids and Basin Evolution (ed. Kyser, K.) 160–196 (Mineralogy Association of Canada, 2000).
- Ballentine, C. J. & Burnard, P. G. Production, release and transport of noble gases in the continental crust. Rev. Mineral. Geochem. 47, 481–538 (2002).
- Bentoumi, G., Didsbury, R., Jonkmans, G., Rodrigo, L. & Sur, B. Direct harvesting of helium-3 (<sup>3</sup>He) from heavy water nuclear reactors. *Nucl. Rev.* 2, 109–112 (2013).
- 33. Shea, D. A. & Morgan, D. The Helium-3 Shortage: Supply, Demand, and Options for Congress (Congressional Research Service, 2010).
- Zartman, R. E., Wasserburg, G. J. & Reynolds, J. H. Helium, argon, and carbon in some natural gases. J. Geophys. Res. 66, 277–306 (1961).

**Publisher's note** Springer Nature remains neutral with regard to jurisdictional claims in published maps and institutional affiliations.

© The Author(s), under exclusive licence to Springer Nature Limited 2022

#### Methods

Delta values definition. We report changes in <sup>4</sup>He/N<sub>2</sub> in delta notation:

$$\delta(^{4}\text{He/N}_{2}) = \frac{(^{4}\text{He/N}_{2})_{SA}}{(^{4}\text{He/N}_{2})_{ST}} - 1 \tag{1}$$

where subscripts SA and ST refer to the ratio in a sample and standard reference gas, respectively.  $\delta(^4{\rm He/N_2})$  is either multiplied by  $10^3$  and reported in 'per mille' units or multiplied by  $10^6$  and expressed in 'per meg' units.

Sampling. We analysed the composition of clean ambient air pumped into pressurized containers by different laboratory groups at irregular times over the past five decades. The samples broadly fall into two groups: those collected in high-pressure cylinders made from aluminium or chrome—molybdenum steel (herein called 'high-pressure cylinders'), and those collected in 34l stainless steel Essex tanks (Essex Cryogenics). The properties of all samples used in this study are detailed in Supplementary Table 1.

Essex tanks. All but one Essex tank were pumped as Advanced Global Atmospheric Gases Experiment standards at either La Jolla or Trinidad Head on an oil-free compressor (RIX Industries, model SA-6B) up to 600–900 psi (4.1–6.2 Mpa) without any purification stage<sup>35,36</sup>. Small amounts of deionized water were added during the filling processes to cool the pump. Essex tank G-038 was filled at Cape Grim using the cryogenic air sampling system described in ref. <sup>3</sup>. Essex tanks are sealed with all-metal valves connected to the tank body using metal-to-metal seals or elastomer-coated national pipe tapered thread. Nine Essex tanks were excluded from this analysis because they exhibit a clear 2–5% positive bias in the helium mole fraction compared with other tanks filled at similar times. For the excluded tanks, no corresponding anomaly is evident in Ar/N<sub>2</sub> or O<sub>2</sub>/N<sub>2</sub>, which suggests that these samples were contaminated with helium at the time of filling. Furthermore, Essex tanks with a remaining pressure below 1.5 MPa were not considered due to an apparent fractionation emerging only at very low pressures (Extended Data Fig. 4).

Aluminium and chrome-molybdenum steel cylinders. All high-pressure cylinders were pumped at Scripps Institution of Oceanography using a separate oil-free compressor (RIX Industries), with additional chemical processing specific to individual tanks. The processing variously included any of the following: passing through high-pressure columns containing Ascarite, Mg(ClO<sub>4</sub>), or 13X molecular sieve, Aquasorb and additions of pure CO<sub>2</sub>, N<sub>2</sub> and O<sub>2</sub>. We expect these modifications to impact only select gases, with generally small or correctable impacts on He/N<sub>2</sub>. The use of 13X molecular sieve was common in the earlier part of the record, but no complete documentation of this is available in the lab notebooks. Air was also temporarily archived on occasion for later use but was typically stored for no longer than a few weeks. Some cylinders contain a blend of air from up to three different sampling dates that was subsequently combined using a diaphragm gas transfer compressor (compresseurs a membrane Corblin, type A1C250). We consider cylinders with multiple fill dates only if they are less than a year apart and assign a representative fill date based on the contribution of each date to the overall cylinder composition. Many of the cylinders have been used to create Northern Hemisphere background records for perfluorocarbons CF<sub>4</sub>, C<sub>2</sub>F<sub>6</sub> and C<sub>3</sub>F<sub>8</sub><sup>37</sup>. We update the fill history of ref. <sup>37</sup> on the basis of additional old logs and lab notebooks. One high-pressure cylinder (LL9082) was filled with the same pumping system used for the Essex tanks and demonstrates the comparability of the two filling systems. We exclude Viton-sealed cylinders from our analysis due to known issues with permeation<sup>38</sup>.

Summary of analysis methods. Our measurements of  ${}^4\mathrm{He/N_2}$  are based on a new mass spectrometric analysis method described in ref.  ${}^{16}$ . The measurement relies on stabilizing the flow of air to a mass spectrometer (MS) to very high precision and monitoring changes in the  ${}^4\mathrm{He^+}$  beam while switching between a sample and reference gas. Variability in the  ${}^4\mathrm{He^+}$  beam can thus be interpreted as a measure of the difference in helium mole fraction between the sample and standard gas. The helium mole fraction measurement can be combined with measured changes in  $O_2/N_2$ ,  $Ar/N_2$  and the  $CO_2$  mole fraction to calculate the change in  ${}^4\mathrm{He/N_2}$  using the equation given by ref.  ${}^{16}$ :

$$\delta(\text{He/N}_2) \approx \delta(\text{He/M}) + \delta(O_2/N_2)X_{O_2} + \delta(\text{Ar/N}_2)X_{\text{Ar}} + dX_{\text{CO}_2}$$
 (2)

where  $\delta(\text{He/M})$  is the helium mole fraction expressed in delta notation following equation (1) with  $M \equiv N_2 + O_2 + Ar + CO_2 + \cdots$ .  $X_{O_2}$  and  $X_{Ar}$  are representative values of the atmospheric oxygen and argon mole fraction, and  $dX_{CO_2}$  denotes the change in the  $CO_2$  mole fraction.

Air is gettered before entry into the MS to remove all non-noble gases and effectively concentrate He by a factor of  $\sim\!100$ . Where available, repeat measurements of He/M were averaged. All samples were measured against the same reference gas cylinder, and He/N $_2$  data are reported relative to the mean of all samples collected in 2020.

The reproducibility of repeat measurements of one standard cylinder over eight months is 26 per meg, but performance of the instrument was not uniform over the period of measurements (Extended Data Fig. 3). Before 25 May 2020 and

following a careful calibration of the inlet system, a reproducibility of 10 per meg was achieved as reported by ref.  $^{16}$ . After 25 May 2020, a lower reproducibility of 29 per meg was obtained. The degradation followed several repairs to the analysis system, including replacement of the sample and standard gas delivery lines to the flow-stabilizing inlet system, replacement of multiple MS electronic parts and replacement of the entire MS source assembly, which required a recalibration of fractionation in the open split. As a conservative estimate, we use the reproducibility of 29 per meg after the repairs as a conservative estimate of  $^4$ He/N $_2$  measurement uncertainty. This precision is more than sufficient to resolve the expected per mille level changes in He/N $_2$  since the 1970s.

Measurements of O<sub>2</sub>/N<sub>2</sub>, Ar/N<sub>2</sub> and CO<sub>2</sub> in high-pressure cylinders were made using instrumentation and methods described by refs. 39,40. These data have a  $1\sigma$  reproducibility of 2 per meg, 3 per meg and 0.03 ppm in  $O_2/N_2$ , Ar/ $N_2$  and CO2, respectively. CO2 readings were taken from a Picarro G2401 analyser for samples with CO2 below 200 ppm due to concerns about the calibration validity of the primary instrumentation at such low CO<sub>2</sub> concentrations. Measurements of O2/N2, Ar/N2 and CO2 in Essex tanks were analysed using the same method but using a second analysis system that included a separate GV Isoprime MS and a Licor Li-6251 CO<sub>2</sub> analyser. The second instrument requires ~10 times less gas for analysis, thus reducing sample usage. Repeatability of O2/N2, Ar/N2 and CO<sub>2</sub> measurements on the second system was 2 per meg, 6 per meg and 0.02 ppm  $(1\sigma)$ , respectively. When applied in equation (2), these errors yield a negligible combined uncertainty in correction from <sup>4</sup>He/M to <sup>4</sup>He/N<sub>2</sub> of 0.4 per meg for both instruments due to the weighting by atmospheric abundance. The secondary MS was calibrated with respect to the primary instrument by repeat measurements of a single standard.

Helium leakage testing. The He/N<sub>2</sub> content of compressed air stored in high-pressure cylinders may potentially have decreased over time due to preferential permeation of He relative to N<sub>2</sub> through elastomeric seals, such as elastomeric valve seats and Teflon tape on pipe threads for the head valves. To quantify the relevant He permeation rates, we exposed the cylinder head valves of several Teflon-sealed and O-ring-sealed cylinders to 1–2 atmospheres of pure helium for 4–6 weeks. This process reverses and amplifies the partial pressure gradient of He between the environment and the cylinder, thus accelerating permeation. A leak sufficient to produce a 1 per meg drift in 1 year during storage would yield a drift of roughly 10 per meg d<sup>-1</sup> in the experiment. Cylinders were analysed before and after exposure to the excess helium, allowing an additional month for the cylinder to rest after exposure before follow-up analysis. The drift rates in the experiment were scaled downwards by the ratio of the natural to amplified helium gradients to assess the expected actual drift rates of these tanks.

The permeation rates for select cylinders are summarized in Extended Data Table 1 and constrain equivalent  ${}^4\text{He/N}_2$  loss rates in our samples to 3 per meg or less per year. This could lead to a drift of up to 120 per meg over 4 decades, which is within the quoted uncertainty. Cylinder ND01645, by contrast, is suspected to have a compromised seal and produced a leak rate of 215 per meg yr $^{-1}$ , demonstrating the sensitivity of our test set-up.

We expect the He/N<sub>2</sub> drift rates of the Essex tanks are comparable to or smaller than that of the high-pressure cylinders. Essex tanks are sealed by all-metal valves connected to the tank body via either metal-to-metal Swagelok connections or Teflon tape seals on pipe threads. Our tests with high-pressure cylinders suggest that Teflon tape produces sufficiently tight seals to prevent problematic drift. Furthermore, we see no evidence in the time series for a dependence of  $^4\mathrm{He/N_2}$  on the seal type (Extended Data Fig. 4).

 $^4\text{He/N}_2$  artefactual fractionation correction. We apply a small correction to  $^4\text{He/N}_2$  data from high-pressure cylinders on the basis of an apparent correlation with biases in  $\text{Ar/N}_2$  compared with true atmospheric concentrations:

$$\delta(^{4}\text{He/N}_{2}) = \delta(^{4}\text{He/N}_{2})_{\text{raw}} + (2.02 \pm 0.12) \times \left[\Delta(\text{Ar/N}_{2}) - \Delta(\text{Ar/N}_{2})_{2020}\right] \tag{3}$$

where  $\delta(^4\text{He/N}_2)_{\text{raw}}$  is the uncorrected He/N<sub>2</sub> observations,  $\Delta(\text{Ar/N}_2)$  is the Ar/  $N_2$  anomaly and  $\Delta (Ar/N_2)_{2020}$  is the mean  $Ar/N_2$  anomaly of cylinders in 2020.  $\Delta(Ar/N_2)$  is defined as the difference between measured values in each cylinder and the true atmospheric value at the time of filling, which was estimated by extrapolating a fit to 15 years of flask data at La Jolla 40 (Extended Data Fig. 5). The correction coefficient is given by the slope of the best-fit line<sup>41</sup> for the relationship between  $\Delta(Ar/N_2)$  and the He/N<sub>2</sub> anomaly  $\Delta(He/N_2)$  (Extended Data Fig. 2). In the absence of a known atmospheric history,  $\Delta(He/N_2)$  is instead defined as the deviation of each sample from a second-order polynomial fit to the uncorrected  $^{4}$ He/N<sub>2</sub> data (Extended Data Fig. 5). For an Ar/N<sub>2</sub> anomaly of 200  $\pm$  6 per meg, the correction adds an uncertainty of 20 per meg (1σ) to our <sup>4</sup>He/N<sub>2</sub> observation. Data from samples with Δ(Ar/N<sub>2</sub>) exceeding 200 per meg are rejected. Essex tank data are uncorrected. A mechanism for the combined fractionation of Ar/ N2 and He/N2 remains unclear. However, similarly correlated Ar/N2 and He/N2 anomalies were observed in an experiment in which cylinders were filled through a 13X molecular sieve, pointing to adsorption as a key process responsible for the artefactual fractionation. Adsorption is also consistent with a near 1:1 relationship observed between  $\Delta(Ar/N_2)$  and  $\Delta(O_2/N_2)$ , where the  $O_2/N_2$  anomaly  $\Delta(O_2/N_2)$  is

defined analogously to  $\Delta(\text{Ar/N}_2),$  but further work would be needed to confirm the adsorption hypothesis.

Uncertainty propagation. We calculate an overall error of 35 per meg ( $1\sigma$ ) for all samples by propagation of uncertainty in quadrature from the initial  $^4{\rm He/M}$  analysis, from the derivation of  $^4{\rm He/N_2}$  and from the artefactual fractionation correction (Extended Data Table 2). This estimate is based on the worst-case scenario of a high-pressure cylinder with the maximum allowed artefactual Ar/N $_2$  fractionation of 200 per meg. Thus, it probably overestimates analytical uncertainty for Essex tanks slightly but allows us to use a consistent conservative uncertainty value for all samples.

#### Data availability

All data generated or analysed during this study are included in the Article. Source data are provided with this paper.

# References

- Prinn, R. G. et al. History of chemically and radiatively important atmospheric gases from the Advanced Global Atmospheric Gases Experiment (AGAGE). Earth Syst. Sci. Data 10, 985–1018 (2018).
- Prinn, R. G. et al. A history of chemically and radiatively important gases in air deduced from ALE/GAGE/AGAGE. J. Geophys. Res. Atmos. 105, 17751–17792 (2000).
- Mühle, J. et al. Perfluorocarbons in the global atmosphere: tetrafluoromethane, hexafluoroethane, and octafluoropropane. *Atmos. Chem. Phys.* 10, 5145–5164 (2010).
- Keeling, R. F., Manning, A. C., Paplawsky, W. J. & Cox, A. C. On the long-term stability of reference gases for atmospheric O<sub>2</sub>/N<sub>2</sub> and CO<sub>2</sub> measurements. *Tellus B* 59, 3–14 (2007).
- Keeling, R. F., Manning, A. C., McEvoy, E. M. & Shertz, S. R. Methods for measuring changes in atmospheric O<sub>2</sub> concentration and their application in Southern Hemisphere air. *J. Geophys. Res.* 103, 3381–3397 (1998).
- Keeling, R. F. et al. Measurement of changes in atmospheric Ar/N<sub>2</sub> ratio using a rapid-switching, single-capillary mass spectrometer system. *Tellus B* 56, 322–338 (2004).

 York, D., Evensen, N. M., Martinez, M. L. & De Basabe Delgado, J. Unified equations for the slope, intercept, and standard errors of the best straight line. *Am. J. Phys.* 72, 367–375 (2004).

# Acknowledgements

We thank R. Beaudette, A. Seltzer, S. Shackleton, J. Morgan, J. Ng, J. Dohner, Y. Jin and E. Morgan for comments and insightful discussions during the development and troubleshooting of the  $He/N_2$  analysis method. We are grateful to S. Hatley, A. Cox and T. Lueker for locating many old cylinders and unearthing documentation of their history. This work would not have been possible without the support of C. Harth, who generously shared the AGAGE Essex tanks and advised on their use and history. We also thank B. Paplawsky and S. Clark for maintaining and operating the  $Ar/N_2$ ,  $O_2/N_2$  and  $CO_2$  analysis systems in the Keeling laboratory. This work was supported by National Science Foundation grants MRI-1920369 (J.S.), OCE-1924394 (J.S.) and AGS-1940361 (R.EK.).

#### **Author contributions**

B.B. carried out the measurements and data analysis with support from B.P., J.S. and R.F.K. B.B. prepared the manuscript, which was subsequently edited by all authors.

# Competing interests

The authors declare no competing interests.

#### Additional information

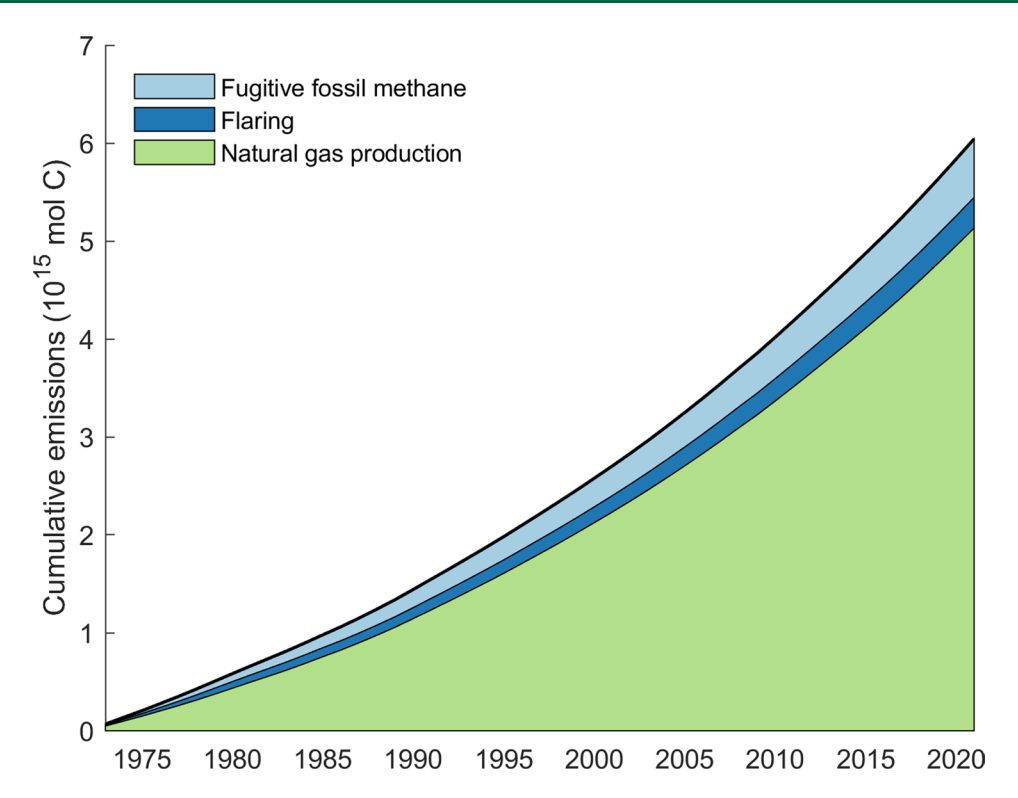
Extended data is available for this paper at https://doi.org/10.1038/s41561-022-00932-3.

**Supplementary information** The online version contains supplementary material available at https://doi.org/10.1038/s41561-022-00932-3.

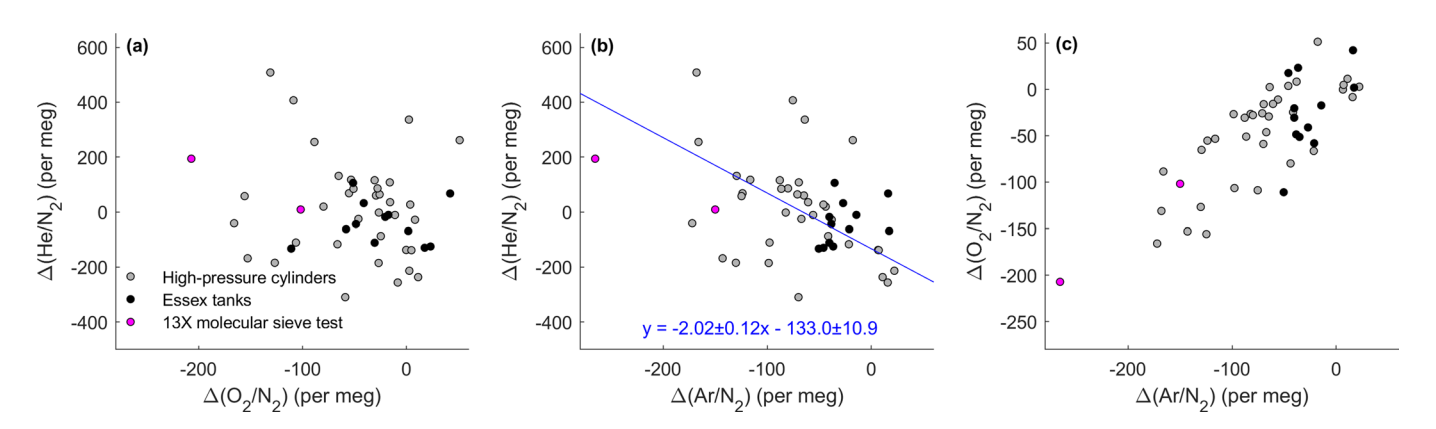
Correspondence and requests for materials should be addressed to Benjamin Birner.

Peer review information Nature Geoscience thanks Yuji Sano, Christine Boucher and the other, anonymous, reviewer(s) for their contribution to the peer review of this work. Primary Handling Editor: Tom Richardson, in collaboration with the Nature Geoscience team.

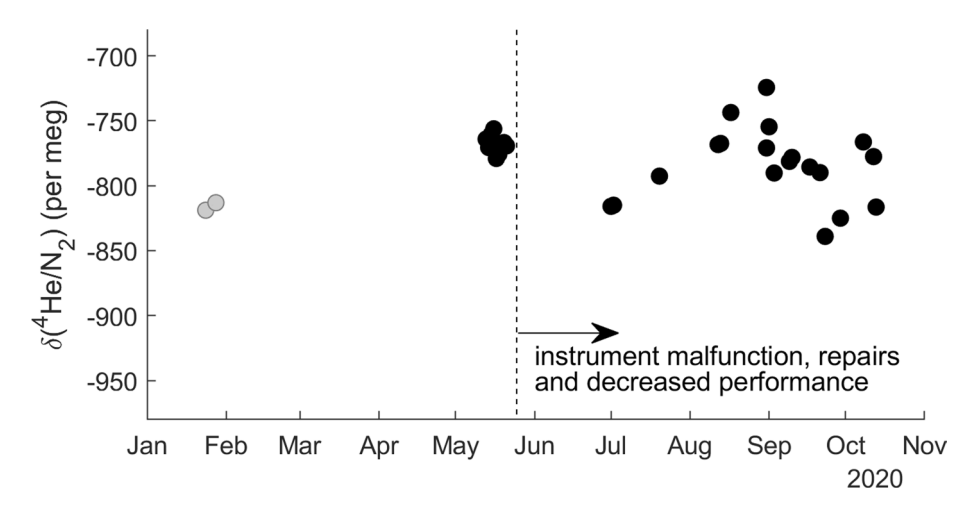
Reprints and permissions information is available at www.nature.com/reprints.



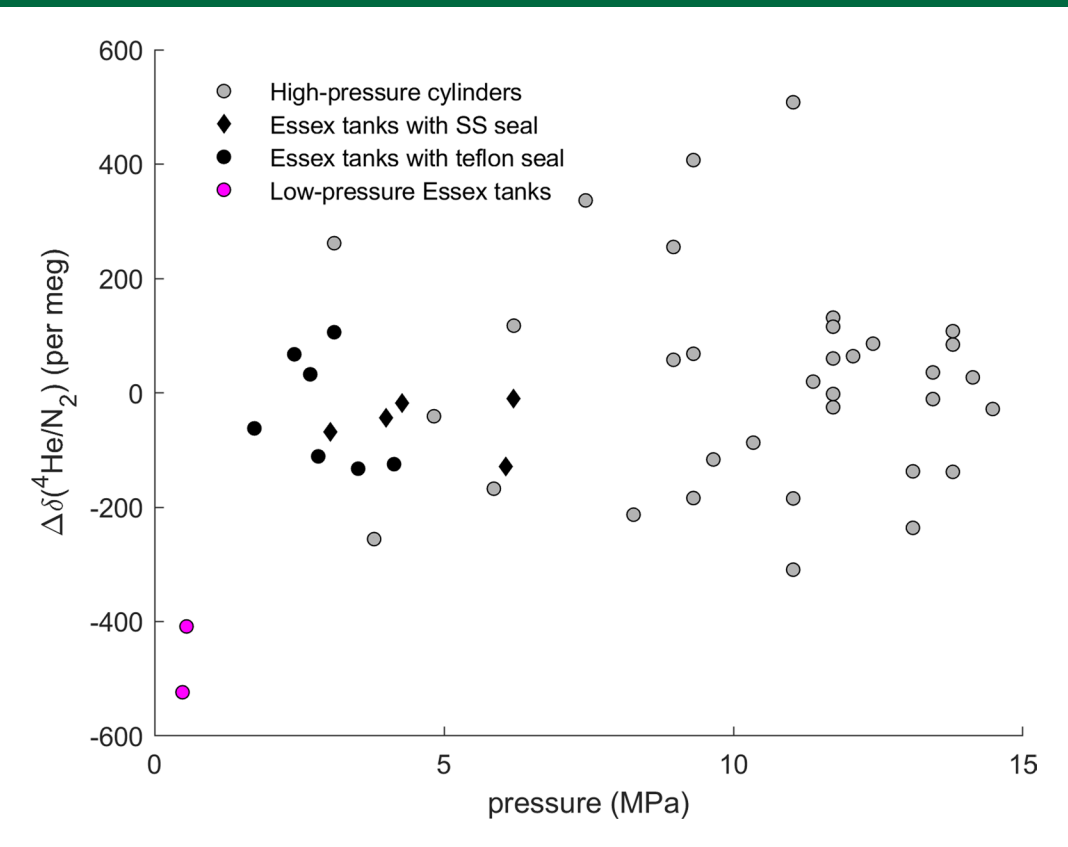
Extended Data Fig. 1 | Cumulative global natural gas emissions from different sources. Data for natural gas production and flaring are from the Global Carbon Budget [42,43]. Data for fugitive fossil  $CH_4$  emissions [44] were rescaled to bring them into agreement with observed mean fossil  $CH_4$  emissions in 2003-2012 reported by Hmiel et al. [45] and multiplied by 1.25 to account for carbon compounds other than  $CH_4$  present in natural gas. All emission records are extrapolated to 2021 using a smoothing spline.



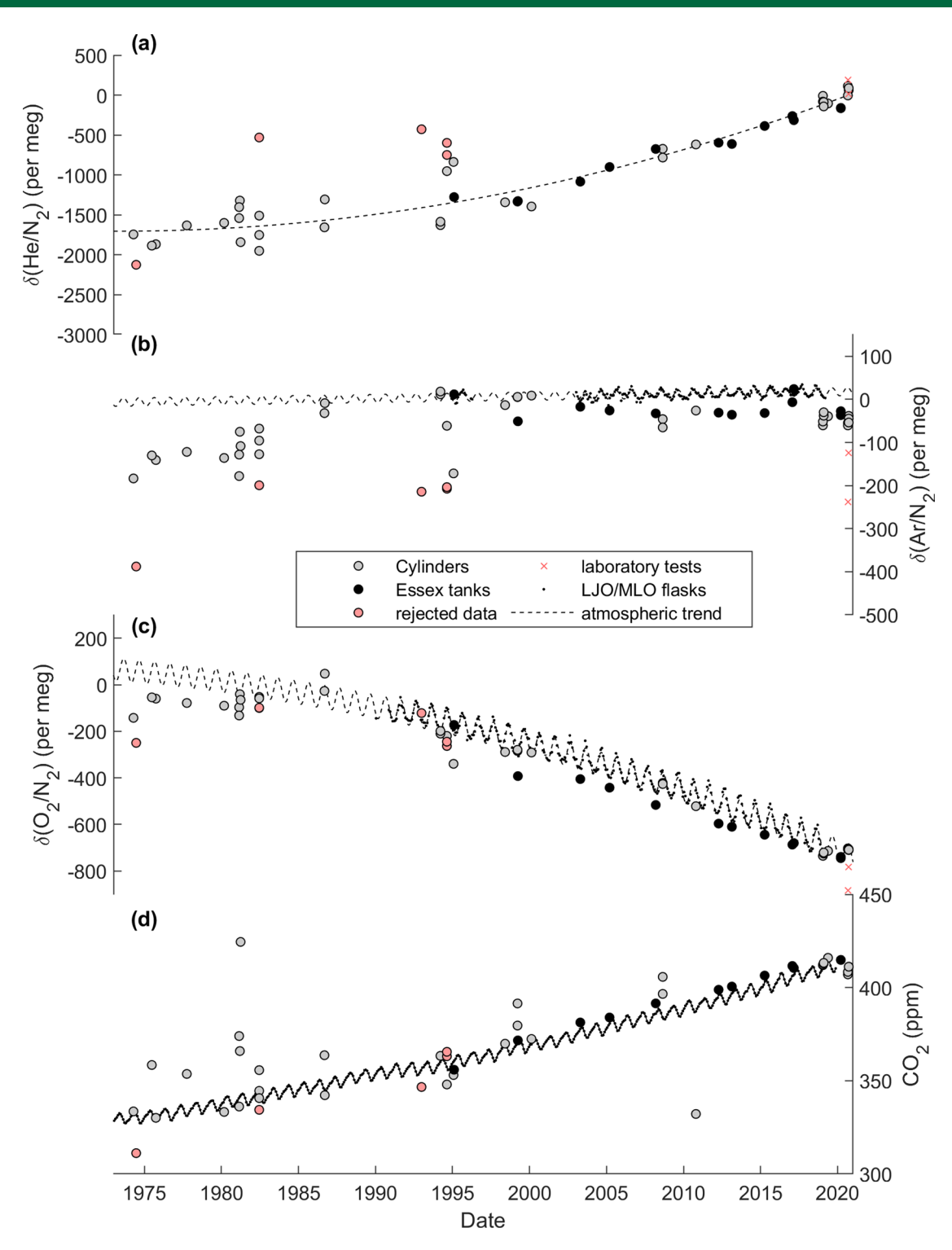
**Extended Data Fig. 2 | Relationships between anomalies in O\_2/N\_2,**  $^4$ He/ $N_2$ , and Ar/ $N_2$ . Anomalies are defined as deviations from the true atmospheric history denoted as  $\Delta(O_2/N_2)$ ,  $\Delta(^4$ He/ $N_2)$ , and  $\Delta(Ar/N_2)$ . Relationships are shown between (a)  $\Delta(O_2/N_2)$  and  $\Delta(^4$ He/ $N_2)$ , (b)  $\Delta(Ar/N_2)$  and  $\Delta(^4$ He/ $N_2)$ , and (c)  $\Delta(Ar/N_2)$  and  $\Delta(O_2/N_2)$ . Best fit lines are calculated using the method of York et al. and exclude data from Essex tanks (black circles). Magenta circles show results from test measurements of cylinders filled through 13X mole sieve which presumably was used as a drying agent at different times in the past.



**Extended Data Fig. 3 | Repeat analysis of the same sample and standard cylinder combination.** Cylinder ND33676 was first measured in January 2020 before the open split biases were calibrated (gray circles) and then analyzed regularly (black circles) to constrain measurement repeatability. Major changes to the analysis system were made at the end of May 2020 and previous performance was never fully recovered as highlighted on the graphic.



**Extended Data Fig. 4 | Relationship between pressure and the {}^4\text{He/N}\_2 anomaly.** The  ${}^4\text{He/N}_2$  anomaly is defined as the difference between the measured  ${}^4\text{He/N}_2$  in each sample and our estimate of the atmospheric change (that is, best fit line in Extended Data Figure 5). Essex tanks (black circles and diamonds) and high-pressure cylinders (gray circles) show no clear pressure dependence above 1.5 MPa. Two Essex tanks (magenta circles) with pressure below 1 MPa are clear outliers and their data are rejected. The  ${}^4\text{He/N}_2$  anomaly in Essex tanks does not vary systematically between tanks using all stainless-steel seals (SS, black circles) and tanks using Teflon tape seals on tapered threads (black diamonds).



**Extended Data Fig. 5 | Uncorrected timeseries of (a) He/N<sub>2</sub>, (b) Ar/N<sub>2</sub>, (c) O<sub>2</sub>/N<sub>2</sub> and (d) CO<sub>2</sub> in our samples.** Monthly means of flask observations from La Jolla (LJO) and Mauna Loa (MLO) are shown for comparison with a polynomial fit of the trend and a one harmonic seasonal cycle. Results from high-pressure cylinders (gray) and Essex tanks (black) are shown separately. Data were quality screen as described in the text and some samples rejected (magenta circles) if  $Ar/N_2$  deviated more than 200 per meg from the fit to flask data (black dotted line). Results from two laboratory tests of drying air with 13X molecular sieve are shown as red crosses.

Cylinder Name	Seal type	Duration (days)	<sup>4</sup> He pressure differential (Pa)	$^4{ m He/N_2}$ change (per meg)	Tank pressure (MPa)	Estimated $^4\mathrm{He/N_2}$ drift rate (per meg y $^{-1}$ )
CDK10068Q	NPT	37.98	1.08E+05	262.32	11.03	1.33
CDK34816Q	NPT	37.98	1.08E+05	446.1	5.38	1.1
CDK3758Q	NPT	37.98	1.08E+05	108.65	9.65	0.48
CDK7357Q	NPT	39.38	2.05E+05	387.71	13.79	1.26
ND33777	NPT	37.98	1.08E+05	154.12	13.79	0.98
cc105762	Metal o-ring	47.06	1.84E+05	1769.4	7.58	2.92
ND01645	Metal o-ring	4.71	2.05E+05	22963	4.83	215.38

**Extended Data Table 1 | Summary of experimental conditions for helium permeation experiments with high-pressure cylinders.** .

Error source	magnitude (per meg)
Reproducibility of repeat <sup>4</sup> He/M measurements	29
Fractionation correction, $\Delta Ar/N_2 = 200 \pm 6$ per meg	20
Derivation of ${}^4\mathrm{He/N_2}$ following Eq. (2)	0.4
Total uncertainty ${}^4{ m He/N_2}$	35

**Extended Data Table 2** | Contributions to the overall uncertainty in  ${}^4\text{He/N}_2$  (1 $\sigma$ ).